Reference hypernetted chain theory for linear molecular fluids: A comprehensive study of the gasliquid coexistence

J. A. Anta, E. Lomba, M. Lombardero, and C. Martín

Articles you may be interested in

Reference hypernetted chain theory for linear molecular fluids: A comprehensive study of the gas-liquid coexistence

J. A. Anta and E. Lomba
Instituto de Química Física Rocasolano, CSIC, Serrano 119, E-28006 Madrid, Spain

M. Lombardero and C. Martín
Instituto de Química Física Rocasolano, CSIC, Serrano 119, E-28006 Madrid and Depto. Química Física I, U. Complutense, E-28040 Madrid, Spain

We have used the reference hypernetted chain theory (RHNC) with a hard-core reference fluid treated in the modified Verlet's approximation (VM) to obtain the gas-liquid coexistence curve of centrosymmetric linear molecular fluids modeled via site-site Lennard-Jones interactions with and without electrostatic forces. Explicit results are presented for the gas-liquid equilibrium of molecular nitrogen and carbon dioxide. Thermodynamic consistency constraints are crucial to define the reference system. Comparison with Gibbs Ensemble Monte Carlo and density functional theory (DFT) calculations evidence the RHNC-VM theory is an excellent tool for predicting coexistence densities and vapor pressures of linear molecular fluids. © *1996 American Institute of Physics.* [S0021-9606(96)50734-8]

I. INTRODUCTION

The RHNC equation is to date one of the best approximations to describe the microscopic structure and equilibrium properties of fluids.[1] Recent developments have extended the range of application of the RHNC theory to linear molecular liquids that interact via site–site Lennard-Jones potentials,[2,3] by making use of Verlet's modified integral equation to calculate the properties of the nonspherical reference system.[4,5] This RHNC-VM equation, as it will be denoted hereafter, yields almost exact results for the spherical harmonic components of the molecular pair distribution function and excellent predictions for fluid thermodynamics. Also, the evaluation of site–site pair distribution functions and atomic structure factors has been successfully accomplished using the RHNC-VM approach in the case of diatomic fluids.[6,7]

On the other hand, the problem of gas–liquid coexistence remains elusive to integral equation calculations. This is due to the fact that the solution of molecular integral equations is very time consuming, specially at high densities and low temperatures, and thus the computation of phase diagrams for realistic molecular potentials has been so far nearly unfeasible. Recently, new and faster solution algorithms have been explored and their performance tested when computing the coexistence curve of homonuclear diatomic fluids in the somewhat simpler hypernetted chain (HNC) approach.[8] These advances together with the improvement of computer facilities have turned the evaluation of gas–liquid coexistence properties by means of the RHNC-VM equation a feasible task. In this work, we will consider site-site Lennard-Jones potentials, which have shown to be very accurate in reproducing the phase equilibrium behavior of a variety of molecular fluids if the potential parameters are conveniently chosen according to the principle of corresponding states.[9,10]

On the other hand an arguable point in the RHNC-VM

formalism lies in the definition of the α-parameter which determines the reference system molecular size.[2] For homonuclear molecules α has been set by fitting the internal energy and compressibility factor to Monte Carlo data in the atomic Lennard-Jones fluid.[2] However, the determination of this parameter for heteronuclear molecules requires a different approach that can account for the different energy and range site–site parameters in the molecule.[3] In this respect, the use of thermodynamic consistency constraints appears as the most flexible choice. Self consistent integral equations have been widely used for simple liquids[11,12] although, to our knowledge, just one single attempt dealing with molecular fluids has been published.[13] Since the self-consistent choice improves significantly the results for the thermodynamic properties of the fluid,[13] a better prediction of the coexistence curve is to be expected.

We have focused this paper towards two main goals. On one hand, we intend to test the ability of the RHNC-VM approximation to calculate properties of linear molecular fluids, in particular when thermodynamic consistency is included, being the determination of the gas–liquid coexistence curve the final and most relevant aim. On the other hand, a more comprehensive study of coexistence properties of systems like N_2 and CO_2 has been carried out, which includes Gibbs Ensemble Monte Carlo (GEMC) simulations and integral equation calculations plus DFT results. The latter have been obtained in a straightforward extension of Frodl and Dietrich's approach.[14] The aforementioned substances have been modeled by means of a three-center Lennard-Jones potential where parameters are summarized in Table I. The rest of the paper is organized as follows. Section II is devoted to recall the essential features of the RHNC-VM theory with special emphasis on the methods used to evaluate the excess free energy. In Sec. III the extension of Frodl and Dietrich's DFT treatment to site–site potentials is presented. Section IV is devoted to present the phase coexist-

ence properties for three different models of N_2 and CO_2. Finally, some conclusions that can be drawn from this work are collected in Sec. V.

II. THE RHNC-VM THEORY

A. General formalism

The core of all RHNC-like theories is the Ornstein–Zernike (OZ) relation, which for molecular fluids can be written in the form

$$\gamma(12) = \frac{\rho}{\omega} \int c(13)[\gamma(32) + c(32)] d3, \tag{1}$$

where $c(12)$ is the direct correlation function between particles 1 and 2, and $\gamma(12)$ is the series function defined as

$$\gamma(12) = h(12) - c(12) \tag{2}$$

being $h(12)$ the total correlation function. ω is the orientational profile whose value is 4π for linear molecules and $8\pi^2$ for nonlinear ones, and ρ is then number density.

The OZ equation has to be solved coupled with an appropriate closure relation which relates both γ and c. In general the closure relation reads

$$c(12) = \exp[-\beta u(12) + \gamma(12) - B(12)] - \gamma(12) - 1, \tag{3}$$

where $u(12)$ is the pair interaction between particles 1 and 2, $\beta = 1/kT$ as usual, and a new function $B(12)$, the so-called bridge function, is introduced. All integral equation theories in the OZ hierarchy can be understood in terms of approximations to this function, the simplest being the hypernetted chain equation which assumes the bridge function to be zero. In the reference hypernetted chain approach the real bridge function of the system is replaced by that of a suitably chosen reference system. The reference system most widely used in RHNC calculations has been the corresponding hard-core system[2,3] for which accurate integral equation approximations are available. Thus the RHNC closure relation reads

$$c(12) = \exp[-\beta u(12) + \gamma(12) - B_o(12)] - \gamma(12) - 1, \tag{4}$$

where $B_o(12)$ is the reference system bridge function.

In hard-core systems, Verlet's semiempirical approach for $B_o(12)$[4] with the improvements of Labik *et al.*[5] has proved to be very accurate in predicting both the thermodynamic properties and the structure of the fluid when soled coupled with the OZ relation. Verlet's Modified bridge function reads

$$B_o(12) = \frac{1}{2} \frac{\gamma_o^2(12)}{1 + a\gamma_o(12)} \tag{5}$$

with

$$a = 1 - \frac{1}{3}\rho d^3, \tag{6}$$

where d the equivalent sphere diameter, that is, the diameter of the sphere whose volume is equal to that of the system molecules. As mentioned before, the combination of the ref-
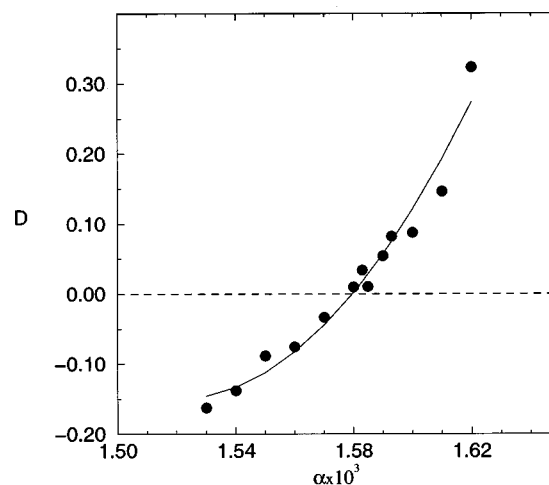

FIG. 1. Plot of D [see Eq. (9) in the text] versus α for the quadrupolar model of CO_2 at $T = 273.15$ K and $\rho = 0.92507$g cm^3. The solid line stands for a least squares fit to a second order polynomial.

erence hypernetted chain equation with a Verlet's modified hard-core bridge function, will be referred to as RHNC-VM.

When performing calculations for molecular liquids described via realistic site–site soft potentials the main problem is always the choice of the reference system, i.e., to find the optimum geometry of the hard-core molecule whose bridge function would lead to sufficiently accurate results for both thermodynamics and correlation functions of the real system when inserted into Eq. (4). In previous works[2,3] it was found that defining the atomic diameters of the reference system as

$$d_i(T,\rho) = \sigma_i \alpha [25 - \ln(kT/\epsilon_i)][25 + \ln(\rho\sigma_i^3)], \tag{7}$$

where σ_i and ϵ_i are the range and well depth potential parameters associated with site i, represents a quasi optimum choice for the reference system. In line with the findings in Ref. 2 and Ref. 3 the reduced bond length or elongation is assumed to be the same in both reference and ''perturbed'' systems, whereas an adjustable parameter α remains undefined. For homonuclear site–site Lennard-Jones potentials the following value for α has been proposed

$$\alpha = 1.620 \times 10^{-3}, \tag{8}$$

which was fixed by fitting the energy and the pressure obtained from the RHNC-VM theory for the monoatomic Lennard-Jones fluid to Monte Carlo results.[2]

When dealing with heteronuclear molecules, the previous value for α does not account properly for the asymmetry of the system and a new empirical approximation closely connected with Eqs. (7) and (8) had to be proposed.[3] Nevertheless, in this work we have decided to explore the use of thermodynamic consistency constraints in order to define α. In short, we have imposed the condition

$$D = \left(\frac{\partial P_v/kT}{\partial \rho}\right)_T^{-1} - \rho kT\chi_T = 0, \tag{9}$$
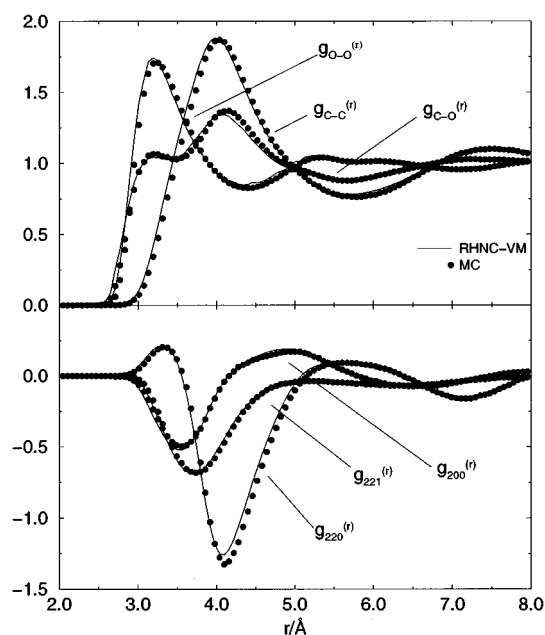
FIG. 2. Site-site radial distribution functions (top) and spherical harmonic components of the molecular pair distribution function (bottom) for the MSM model of CO_2 at 218 K and 1.172g cm^{-3}. Solid lines represent RHNC-VM results with $\alpha = 1.58 \times 10^{-3}$ and black circles MC results.

$$\gamma(12) = 4\pi \sum_{m=0}^{\infty} \sum_{l_1,l_2=m}^{\infty} \gamma_{l_1 l_2 m}(r_{12}) Y_{l_1 m}(\theta_1, \phi_1)$$

$$\times Y_{l_2 \bar{m}}(\theta_2, \phi_2). \qquad (10)$$

Two main obstacles arise in the implementation of a general method for solving integral equations for realistic molecular models, specially if the final aim is the computation of the gas liquid coexistence curve. The first of them is the evaluation of the closure relation, which for molecular fluids is a very time consuming task. In this respect the hybrid method introduced in Ref. 8, as far as systems without center of symmetry are concerned, is not useful anymore since terms with $l_1 + l_2$ odd cannot be neglected in the expansion (10) and the number of coefficients whose couplings have to be calculated becomes intractably large. Therefore, the standard multidimensional integration with Orszag's fast-transform algorithm[8] was adopted as the general procedure for computing the angular projections of the closure. Furthermore, a remarkable decrease of computer time can be accomplished at expenses of larger storage usage if the intermolecular potential is stored in a large multidimensional array.

A second shortcoming when solving the RHNC-VM integral equation is the poor convergence of the original Picard's iterative process at high densities and low temperatures. This limitation can be tackled with by use of Ng's acceleration[17] which has proved to be very efficient in reducing the total number of iterations needed to achieve convergence. As an example, in Table II we report CPU times needed to solve the integral equation for some thermodynamic states located on the liquid side of the coexistence curve. Ng's algorithm makes possible to reach these points in only two stages: first solving for a supercritical state at the desired density starting from an ideal gas solution ($\gamma(12) = 0$) and then cooling the system at constant density down to the desired temperature.

where χ_T is the isothermal compressibility as obtained via the compressibility equation and P_v is the calculated virial pressure. To be rigorous Eq. (9) should be applied for each temperature and density, although as in Ref. 2 and Ref. 3 we found that α is sort of an universal parameter, and hence an unique value of α may be used for a whole set of computations. Fig. 1 illustrates the way in which the α parameter was determined.

In Table II RHNC-VM results are compared with MC data. In particular, for liquid CO_2 it can be seen that a value for α chosen by imposing Eq. (9) leads to a better agreement with the simulation for both a quadrupolar model (or MSM)[15] and a point charge model (or HY).[9] This improvement will be very significant when computing the gas–liquid coexistence curve.

With regard to the site–site pair distribution functions and the spherical harmonic components of the molecular pair distribution function the choice of α is not so relevant and the prediction of the RHNC-VM approximation reproduces remarkably well the distribution functions obtained from simulation for different values of α. In Fig. 2 this good agreement between theory and simulation can be clearly observed.

C. Evaluation of the free energy

A common problem in integral equation theories is the calculation of the Helmholtz free energy of the fluid since in most cases one lacks closed and direct expressions that enable its evaluation from the correlation functions. One exception is the HNC approximation, for which the following relation is available[8,16]

$$\frac{A_{HNC}^{ex}}{NkT} = \frac{1}{2}\rho(\beta/\rho\chi_T - 1) - \frac{1}{2\rho}\int \left\{ \rho^2 \sum_{l_1 l_2 m} \tilde{h}_{l_1 l_2 m}(k) \right.$$

$$\times \left(\frac{1}{2}\tilde{h}_{l_1 l_2 m}(k) - \tilde{\gamma}_{l_1 l_2 m}(k) \right)$$

$$+ \sum_m \log \text{Det}[\mathbf{I} + (-1)^m \rho \tilde{\mathbf{H}}_m(k)]$$

$$\left. - (-1)^m \rho \, \text{Tr} \tilde{\mathbf{H}}_m(k) \right\} \frac{d\mathbf{k}}{(2\pi)^3}, \qquad (11)$$

B. Method of solution

The method for solving Eqs. (1) and (4) for both reference and real systems has already been described in full elsewhere[8,16] and is based on the expansion of the pair functions in spherical harmonics

where $\widetilde{\mathbf{H}}_m$ is a matrix whose elements are $[\widetilde{\mathbf{H}}_m]_{l_1 l_2} = \widetilde{h}_{l_1 l_2 m}$ for $l_1, l_2 \geq m$ and the tilde denotes a three-dimensional Fourier transform.

As to the RHNC theory, it can be shown[16] that it is possible to approximate the excess free energy by means of

$$\frac{A^{\text{ex}}}{NkT} \simeq \frac{A^{\text{ex}}_{\text{HNC}}}{NkT} - \frac{A^{(o)}_{\text{HNC}}}{NkT} + \frac{A^{(o)}}{NkT} \qquad (12)$$

$$\frac{A^{(o)}}{NkT} = \frac{(3\alpha + \alpha^2)\eta - 3\alpha^2 \eta^2 + \ln(1-\eta)[\alpha^2 - 1 + (2 - 2\alpha^2)\eta + (\alpha^2 - 1)\eta^2]}{(1-\eta)^2}, \qquad (13)$$

where η is the system packing fraction and α [not to be mistaken with that of Eq. (7)] is the parameter of nonsphericity

$$\alpha = \frac{RS}{3V} \qquad (14)$$

being S and V the surface and the volume of the molecule respectively, and R the mean curvature integral divided by 4π. Expressions to calculate these magnitudes for hard-core linear molecules are available in the literature.[19] Note that if the reference system is calculated in the VM approximation, to be consistent, one should also calculate $A^{(o)}$ in the same approximation. Unfortunately, closed expressions for the VM excess free energy are not available and we have thus resorted to Eq. (13).

The free energy can be also evaluated by thermodynamic integration of the compressibility factor and/or the internal energy. If the state lays in the gas region we will then use the expression

$$\frac{A^{ex}(\rho, T)}{NkT} = \int_0^\rho \left(\frac{P_v(\rho', T)}{\rho' kT} - 1 \right) \frac{d\rho'}{\rho'}. \qquad (15)$$

When dealing with the liquid phase, a more elaborated procedure is required, which involves an integration of $P/\rho kT$ along a supercritical isotherm plus an integration of the internal energy along an isochore

$$\frac{A^{\text{ex}}(\rho, T)}{NkT}$$

$$= \int_0^\rho \left(\frac{P_v(\rho', T_s)}{\rho' kT_s} - 1 \right) \frac{d\rho'}{\rho'} + \int_{T_s}^{T} - \frac{U(\rho, T')}{NkT'} \frac{dT'}{T'}, \qquad (16)$$

where T_s is a temperature higher than the system critical temperature.

Both methods to compute A^{ex}/NkT are compared in Fig. 3 for the liquid portion of an isotherm. Excess free energy computed via thermodynamic integration is always higher than that obtained by applying Eq. (12). This might be due to the use of Eq. (13) instead of the proper VM hard-core excess free energy, or more likely to the intrinsic thermody-

being $A^{\text{ex}}_{\text{HNC}}$ and $A^{(o)}_{\text{HNC}}$ the excess free energy as computed via Eq. (11) for the real and reference system respectively and $A^{(o)}$ the exact excess free energy for the reference system. As already mentioned most RHNC calculations rely on the hard-core fluid as a reference system. In the case of nonspherical hard-core systems, an almost exact expression for computing $A^{(o)}/NkT$ is available[18]

namic inconsistency of the closure. We will see later the influence of this discrepancy on the RHNC-VM phase coexistence line.

III. DENSITY FUNCTIONAL THEORY FOR MOLECULAR SITE-SITE LENNARD-JONES MODELS

We have extended Frodl and Dietrich's formalism[14] to molecular liquids with a nonspherical core. Essentially, the central problem in the DFT in the modified mean field (MMF) approximation is the evaluation of the integral

$$W(T) = \frac{4\pi}{\beta} \int e^{-\beta U_{\text{ref}}(12)} (1 - e^{-\beta U_{\text{ex}}(12)}) d1 d2, \qquad (17)$$

where $U_{\text{ref}}(12)$ and $U_{\text{ex}}(12)$ are respectively the reference and excess parts of the full interaction potential

$$U(12) = U_{\text{ref}}(12) + U_{\text{ex}}(12). \qquad (18)$$

Since our potential is a sum of site–site interactions we have applied Barker–Henderson's decomposition[20] to each of them

$$u_{ij}^{\text{ref}}(r_{ij}) = \begin{cases} u_{LJ}(r_{ij}), & r_{ij} < \sigma_{ij} \\ 0, & r_{ij} > \sigma_{ij} \end{cases} \qquad (19)$$
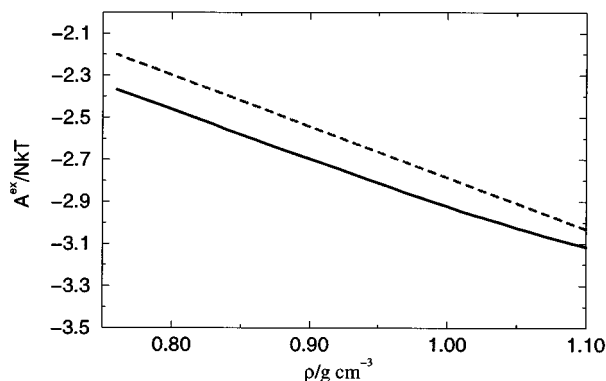

FIG. 3. Excess free energy as computed via Eqs. (12) (solid line) and (16) (dashed line) for N_2 at 243.15 K.

TABLE I. Models studied in this work.

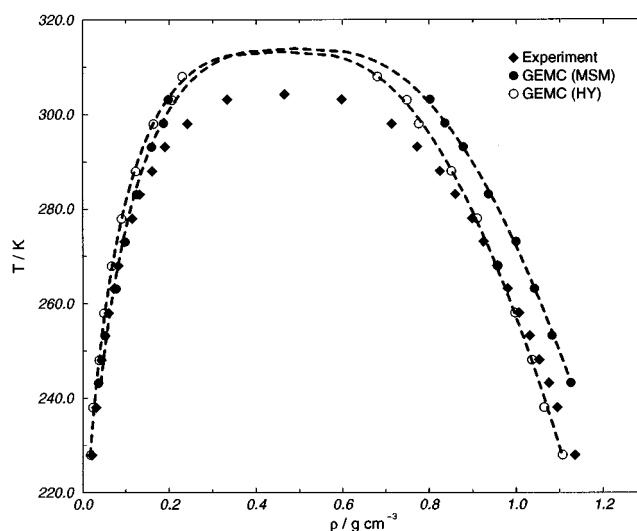|	ϵ/K	$\sigma/\text{Å}$	$L/\text{Å}$
	N_2 (Ref. 15)		
N–N	37.300	3.310	1.090
	CO_2 (MSM model) ($Q=-3.85D\text{Å}$) (Ref. 16)		
C–C	29.000	2.785	-
O–O	83.100	3.014	-
C–O	49.100	2.899	1.160
	CO_2 (HY model) ($q_C=+0.6512$) (Ref. 9)		
C–C	28.129	2.757	-
O–O	80.507	3.033	-
C–O	47.588	2.892	1.149

FIG. 4. Experimental gas–liquid coexistence data of carbon dioxide taken from Ref. 24 and those predicted by MSM and HY models of CO_2 as computed from GEMC simulations. Dashed lines mean the same as in Fig. 5.

$$u_{ij}^{ex}(r_{ij})=\begin{cases} 0, & r_{ij}<\sigma_{ij} \\ u_{LJ}(r_{ij}), & r_{ij}>\sigma_{ij} \end{cases} \quad (20)$$

with

$$u_{LJ}(r_{ij})=4\epsilon_{ij}\left[\left(\frac{\sigma_{ij}}{r_{ij}}\right)^{12}-\left(\frac{\sigma_{ij}}{r_{ij}}\right)^{6}\right]. \quad (21)$$

When the system is bestowed with electrostatic interactions, they are then included in the excess part of the potential. Following Barker and Henderson's approach, the reference potential is replaced by a hard-core potential with the same geometry as the original system, which in our case we select in such a way that its second-virial coefficient is the same as that of the soft-core reference system, i.e.

$$\int (e^{-\beta U_{ref}(12)}-1)d1d2=\int (e^{-\beta U_{hc}(12)}-1)d1d2. \quad (22)$$

Since the second-virial coefficient of a hard-core molecule depends on its volume we can assure fulfillment of Eq. (22) by scaling the distances and atomic sizes in the hard-core reference system. Bearing this in mind Eq. (17) now reads

$$W(T)=\frac{4\pi}{\beta}\int E(12;T)(1-e^{-\beta U_{ex}(12)})d1d2 \quad (23)$$

being $E(12;T)$ equal to 0 for those orientations for which hard-core molecules 1 and 2 overlap and equal to 1 otherwise. The multidimensional integration can simply be handled by standard quadrature methods like those implemented to evaluate the angular projections of the closure (4). (For more details see Ref. 8.)

Once $W(T)$ is determined for a given temperature, both pressure and chemical potential will be calculated via

$$P=-A_{hc}-\frac{1}{2}\rho^2 W(T)+\mu\rho, \quad (24)$$

$$\mu=\frac{\partial A_{hc}}{\partial\rho}-W(T)\rho, \quad (25)$$

where A_{hc} is the free energy of the hard-core system, which can be obtained using Eq. (13).

IV. GAS-LIQUID COEXISTENCE LINE

A. Models and simulation in the Gibbs ensemble

Three site–site Lennard-Jones models have been dealt with in this work (see Table I), one of them for molecular nitrogen and two for carbon dioxide. In order to assess the performance of the RHNC-VM approach in predicting coexistence properties, GEMC simulations[10,21] were carried out to compute the phase diagram of N_2 with the model of Cheung and Powles,[22] and CO_2 with the quadrupolar model

TABLE II. Summary of results obtained from RHNC-VM theory compared with NVT MC data. CPU times needed to solve the integral equation for the thermodynamics states indicated starting from an initial zero-density solution in a DEC AlphaStation 200 are also shown in the table. MC computations for these models were performed with 250 particles and 12000 total steps, including 2000 steps for equilibration.

Model	$\alpha\times10^3$	T/K	$\rho/\text{g cm}^{-3}$	$U/Kj\ \text{mol}^{-1}$	P/Kbar	CPU Time/s	$U/Kj\ \text{mol}^{-1}$(MC)	P/Kbar(MC)
N_2	1.620	99.42	0.7	−4.335	−0.009	235	−4.34	0.0081
CO_2(MSM)	1.620	273.15	0.92507	−10.493	−0.153	319	−10.63	−0.075
CO_2(MSM)	1.580[a]	273.15	0.92507	−10.513	−0.069	286	−10.63	−0.075
CO_2(HY)	1.620	273.15	0.92507	−10.805	−0.067	302	−10.88	0.020
CO_2(HY)	1.595[a]	273.15	0.92507	−10.809	−0.0035	294	−10.88	0.020

[a]Value obtained by applying Eq. (9).

TABLE III. Phase coexistence results for N_2 as obtained from GEMC simulations and RHNC-VM theory with $\alpha = 1.62.10^{-3}$. Labels (1) and (2) indicate that free energy has been calculated via Eqs. (12) and (16) respectively.

	GEMC				RHNC-VM (1)			RHNC-VM (2)		
T/K	ρ_g/g cm^{-3}	ρ_l/g cm^{-3}	P_g/Kbar	P_l/Kbar	ρ_g/g cm^{-3}	ρ_l/g cm^{-3}	P/Kbar	ρ_g/g cm^{-3}	ρ_l/g cm^{-3}	P/Kbar
64.79	0.00094(17)	0.8571(8)	0.00018(4)	−0.00090(230)	0.00147	0.86369	0.00028	0.00052	0.86366	0.00010
78.06	0.00535(11)	0.8027(72)	0.00118(4)	0.00105(602)	0.00961	0.80673	0.00204	0.00378	0.80644	0.00085
90.64	0.01719(128)	0.7447(26)	0.00412(37)	0.00434(341)	0.03476	0.75070	0.00693	0.01079	0.74925	0.00269
99.42	0.03145(103)	0.7010(18)	0.00767(25)	0.00809(546)	0.08768	0.70915	0.01064	0.02130	0.70690	0.00553
111.95	0.07063(180)	0.6228(23)	0.01624(43)	0.01526(170)	⋯	⋯	⋯	0.04688	0.64065	0.01233
119.50	0.1279(18)	0.5699(51)	0.02433(85)	0.02428(170)	⋯	⋯	⋯	0.10152	0.59415	0.01904

of Murphy, Singer and McDonald (MSM).[15] For the point charge model of Harris and Yung (HY) coexistence properties were already available in the literature.[9]

Our GEMC simulations were performed using 500 particle samples. Simulations were organized in Monte Carlo steps, each step involving a translation and a rotation for every molecule, a change of volume and N_i insertion attempts, that is, interchanges of particles between the two boxes involved in the simulation. Since the probability of interchanging molecules is rather small at high densities, the lower the temperature the larger the value of N_i that must be used. Hence, insertion attempts ranged from 500 (low temperatures) to 25 (high temperatures). The number of steps needed to achieve equilibration ranged from 2000 at low temperatures to 20000 steps at the highest ones. Coexistence densities, pressures and energies were averaged typically over 20000–75000 steps. A good agreement between the averaged pressures of both gas and liquid phases could be observed for all models studied.

In Fig. 4 a comparison of the gas–liquid coexistence lines for the two potentials used to model CO_2 is presented. We can see that both potentials are almost equivalent as far as critical properties are concerned although the point charge model of Harris and Yung predicts more accurately the experimental liquid branch.

B. The RHNC-VM gas–liquid coexistence

RHNC-VM coexistence curves for all the models considered have been computed by performing calculations along isotherms in both the gas and liquid regions of the phase diagram. Besides, a supercritical isotherm and a liquid isochore are required in order to evaluate the excess free energy via Eqs. (15) and (16). Values for the pressure, internal energy and free energy were stored for all these isotherms. The total CPU time required to perform the whole job was typically of 15–20 hours in a DEC Alpha AXP/200. This is approximately half the time needed to perform a single GEMC simulation for just one temperature.

Once isotherm data have been stored, equilibrium densities and vapor pressure can be determined by applying the conditions of chemical equilibrium

$$\left. \begin{array}{l} \beta\mu(\rho_l,T)/N = \beta\mu(\rho_g,T)/N \\ \beta P_v(\rho_l,T)\sigma^3 = \beta P_v(\rho_g,T)\sigma^3 \end{array} \right\}, \tag{26}$$

where μ is the chemical potential, which is calculated through

$$\beta\mu/N = \ln \rho + A^{\mathrm{ex}}/NkT + P_v/\rho kT + f(T). \tag{27}$$

In the expression above, $f(T)$ is a temperature-dependent function that can be neglected in a isothermal construction.

Following this procedure we have computed the coexistence properties presented in Tables III, IV and V and Figs. 5, 6 and 7. As a whole, RHNC-VM theory reproduces reasonably well the coexistence properties of the fluid, although the predicted critical points lay always above the GEMC estimate. Both simulation and theoretical data were fitted to the following equations

$$(\rho_l - \rho_g) = A(T - T_c)^\beta, \tag{28}$$

$$\frac{\rho_l + \rho_g}{2} = \rho_c + B(T - T_c) \tag{29}$$

TABLE IV. Phase coexistence properties for the MSM model of CO_2. Free energies in RHNC-VM calculations were derived using direct expression Eq. (12).

	GEMC				RHNC-VM ($\alpha = 1.62.10^{-3}$)			RHNC-VM ($\alpha = 1.58.10^{-3}$)		
T/K	ρ_g/g cm^{-3}	ρ_l/g cm^{-3}	P_g/Kbar	P_l/Kbar	ρ_g/g cm^{-3}	ρ_l/g cm^{-3}	P/Kbar	ρ_g/g cm^{-3}	ρ_l/g cm^{-3}	P/Kbar
243.15	0.037(1)	1.125(4)	0.0145(8)	0.0146(70)	0.022	1.142	0.0093	0.022	1.094	0.0092
253.15	0.052(2)	1.082(4)	0.0201(4)	0.0207(67)	0.031	1.106	0.0130	0.031	1.058	0.0130
263.15	0.078(1)	1.042(4)	0.0286(10)	0.0289(50)	0.042	1.067	0.0178	0.042	1.019	0.0178
273.15	0.099(5)	0.999(5)	0.0347(10)	0.0374(67)	0.056	1.029	0.0238	0.055	0.979	0.0236
283.15	0.124(3)	0.937(2)	0.0433(28)	0.0420(38)	0.074	0.985	0.0312	0.073	0.934	0.0309
293.15	0.159(9)	0.879(9)	0.0530(50)	0.0597(47)	0.097	0.942	0.0402	0.094	0.886	0.0396
303.15	0.198(5)	0.802(3)	0.0641(20)	0.0667(42)	0.125	0.891	0.0506	0.121	0.835	0.0498

TABLE V. Phase coexistence properties for the HY model of CO_2 from GEMC simulations (Ref. 9) and RHNC-VM theory with $\alpha = 1.595 \times 10^{-3}$. Equation (12) was used to compute free energies.

	GEMC			RHNC-VM		
T/K	ρ_g/g cm^{-3}	ρ_l/g cm^{-3}	P/Kbar	ρ_g/g cm^{-3}	ρ_l/g cm^{-3}	P/Kbar
228	0.019(1)	1.106(2)	0.0076(3)	0.014	1.099	0.0056
238	0.024(2)	1.064(4)	0.0095(8)	0.020	1.067	0.0081
248	0.038(2)	1.036(2)	0.0149(8)	0.027	1.033	0.0115
258	0.049(1)	0.997(3)	0.0198(4)	0.038	0.996	0.0158
268	0.067(2)	0.957(3)	0.0262(7)	0.050	0.959	0.0212
278	0.090(7)	0.910(3)	0.0344(10)	0.066	0.918	0.0278
288	0.123(3)	0.851(4)	0.0450(11)	0.086	0.874	0.0358
298	0.164(1)	0.776(9)	0.0560(10)	0.112	0.795	0.0456
303	0.207(7)	0.749(5)	0.0638(5)	0.127	0.795	0.0509
308	0.230(3)	0.680(5)	0.0724(5)	0.145	0.763	0.0569

being T_c and ρ_c the critical temperature and critical density respectively. The critical exponent β was set to 1/3 in all cases.

For N_2 a value of $\alpha = 1.62 \times 10^{-3}$ has been used to compute the phase diagram and the results are displayed in Table III and Fig. 5. Both thermodynamic integration and formulae (11)–(13) were employed to evaluate the excess free energy. The poor performance of the latter approach translates into its inability to determine coexistence properties above $T = 100$ K. The lack of accuracy of the chemical potential evaluated from Eq. (12) reflects mainly on the gas branch of the coexistence curve, which even intersects the nonsolution line of the integral equation. Thermodynamic integration by contrast allows the determination of the entire curve, yielding a critical temperature of 134.9 K and a critical density of 0.306 g cm^{-3}. GEMC estimates of these quantities are 129.0 K and 0.324 g cm^{-3}. It can readily be seen that thermodynamic integration significantly corrects the location of

the gas branch of the coexistence curve, as well as the predicted vapor pressures, whereas the coexistence liquid densities remain approximately unchanged.

For the quadrupolar model of CO_2 (MSM), two set of isotherms were run, with the α parameter set to 1.62×10^{-3} and 1.58×10^{-3} respectively. This second value was obtained by requiring thermodynamic consistency [Eq. (9)] at $T = 273$ K and $\rho = 0.92507$ g cm^{-3}. The value thus computed was then assumed universally valid for this model of CO_2. In Fig. 6 and Table IV coexistence properties for each value of α are compared. It can be observed that the use of the thermodynamic consistency criterion for adjusting the α-parameter leads to a better prediction of the liquid branch, although gas densities and vapor pressures remain essentially the same. Again it was necessary to resort to thermodynamic integration to evaluate the chemical potential in order to get accurate results, as already found for N_2.
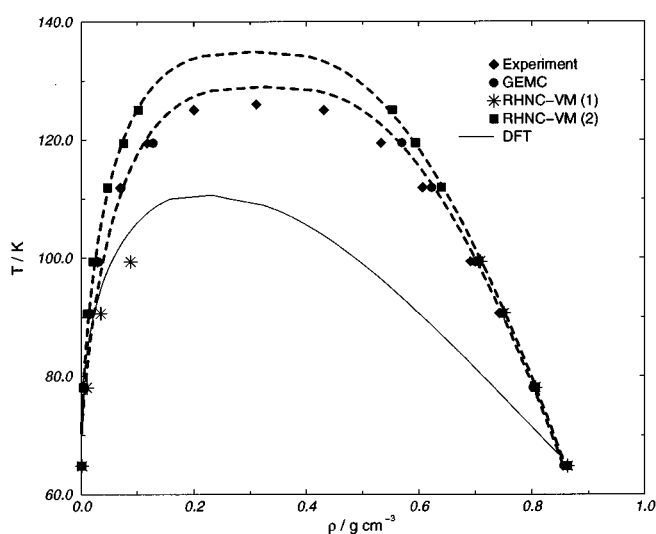

FIG. 5. Gas-liquid coexistence lines for N_2. RHNC-VM data labeled (1) were obtained using Eq. (12) to compute the free energy whereas for those labeled (2) Eqs. (15) and (16) were employed. Dashed lines represent fits to scaling laws with critical exponent $\beta = 1/3$ and the solid line is the prediction of the DFT.
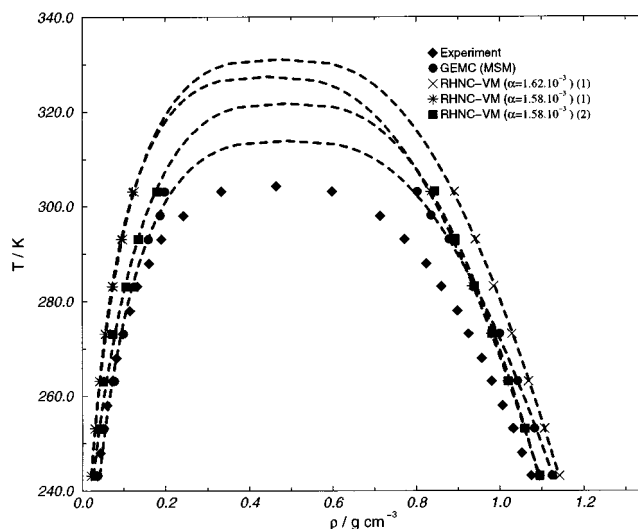

FIG. 6. Experimental gas–liquid coexistence line of carbon dioxide (taken from Ref. 24, prediction from GEMC simulations with model MSM of CO_2, and RHNC-VM curves for the same model computed with different values of α and procedures to compute the free energy [in (1) Eq. (12) was used and in (2) Eqs. (15) and (16)]. Dashed lines denote the same as in Fig. 5.
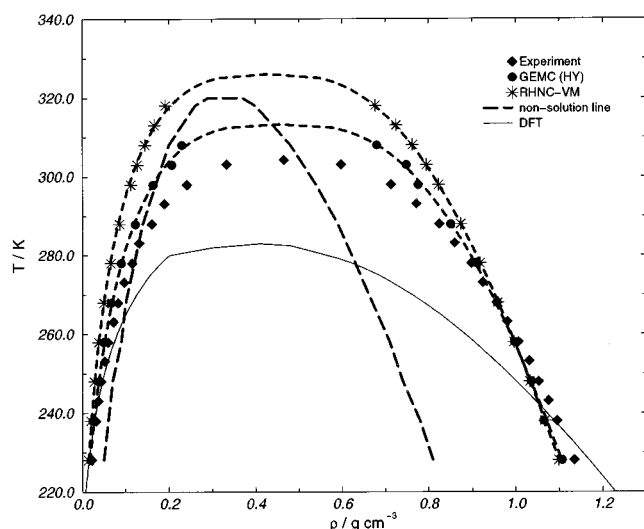
FIG. 7. Experimental phase coexistence properties of carbon dioxide taken from Ref. 24 and those obtained for the HY model of CO_2 from GEMC simulations, RHNC-VM theory with $\alpha = 1.595.10^{-3}$, and DFT. Short-dashed lines stand for fits of data to scaling laws with critical exponent $\beta = 1/3$ and long-dashed line is the non-solution line of RHNC-VM equation. Note: excess free energy in RHNC-VM calculations was evaluated via Eq. (12).

A similar procedure to fix α was applied for the second CO_2 model, which is Harris and Yung's (HY) three-center Lennard-Jones with embedded point charges.[9] Most significant results are collected in Table V and Fig. 7. As in the case of the MSM model, the thermodynamic consistency of Eq. (9) was inforced only once, and for the same thermodynamic state, i.e., $T = 273$ K and $\rho = 0.92507$ g cm^{-3}. Again the calculated $\alpha = 1.595 \times 10^{-3}$ was kept fixed along all isotherms needed to determine the coexisting states. Results show the same good agreement with GEMC data as for the previous models, being the calculated critical point $T_c = 326.1$ K and $\rho_c = 0.429$ g cm^{-3}. (Simulated estimates were $T_c = 312.8$ K and $\rho_c = 0.449$ g cm^{-3}.[9]) In this latter instance we have also determined the nonsolution region of the RHNC-VM equation. It must be pointed out that this region lays completely inside the computed coexistence curve and this fact makes feasible the determination of phase equilibrium states for the whole temperature range. The RHNC-VM theory proves thus to be well-behaved in this regard, mainly when compared with the HNC approximation, for which the coexistence curve not only is rather poor, but is also incomplete due to the crossover with the non-solution line.[8] On the other hand, one should not go as far as to characterize this as a general feature of the RHNC-VM approach. It is well known that the relative location of non-solution, spinodal (if existent) and binodal curves is extremely system dependent.[23]

For completeness we have also calculated the coexistence line using DFT in the modified mean field approximation.[14] This method is not time-consuming compared with RHNC-VM calculations, but unfortunately performs much worse. One might appreciate from Figures 5 and 7 that DFT results deviate in the same way as they do in polar soft spheres[14] although to a much larger extent, as one may expect from the larger anisotropy of these molecular systems.

V. CONCLUDING REMARKS

The RHNC-VM approach has been applied to a homonuclear diatomic molecule and a heteronuclear centrosymmetric triatomic in order to determine the gas–liquid coexistence curve. The present development of integral equation solution methods makes feasible the evaluation of these phase diagrams in a reasonable amount of time and therefore accurate closures of the OZ equation as the RHNC-VM prove to be an interesting tool for computing phase coexistence properties. A thermodynamic consistency criterion to determine the α parameter plus thermodynamic integration to calculate the free energy is the best combination to obtain accurate coexistence properties. Critical temperatures are nonetheless overestimated by a five percent. More accurate results might be expected if the criterion of thermodynamic consistence were used for each thermodynamic state, though this would lead to unreasonably large CPU times. On the other hand, predictions obtained with the simpler modified mean field approximation are quite poor, proving that the good performance of this approach seen in previous works[14] for Stockmayer fluids does not hold for systems with highly non-spherical cores.

As to future developments, the treatment of highly polar, non-centrosymmetric molecular fluids is currently under investigation and will be the subject of a forthcoming publication.

[1] J. P. Hansen and I. R. McDonald, *Theory of Simple Liquids* (Academic, New York, 1986).
[2] M. Lombardero, C. Martín, and E. Lomba, J. Chem. Phys. **97**, 2724 (1992).
[3] M. Lombardero, C. Martín, and E. Lomba, Mol. Phys. **81**, 2724 (1994).
[4] L. Verlet, Mol. Phys. **41**, 183 (1980).
[5] S. Labík, A. Malijevský, and W. R. Smith, Mol. Phys. **73**, 87 (1991).
[6] C. Martín. M. Lombardero, M. Alvarez, and E. Lomba, J. Chem. Phys. **102**, 2092 (1995).
[7] M. Alvarez, E. Lomba, C. Martín, and M. Lombardero, J. Chem. Phys. **103**, 3680 (1995).
[8] J. A. Anta, E. Lomba, C. Martín, M. Lombardero, and F. Lado, Mol. Phys. **84**, 743 (1995).
[9] J. G. Harris and K. H. Yung, J. Phys. Chem. **99**, 12021 (1995).
[10] B. Garzón, S. Lago, C. Vega, E. De Miguel, and L. F. Rull, J. Chem. Phys. **101**, 4166 (1994).
[11] Y. Rosenfeld and N. W. Ashcroft, Phys. Rev. A **20**, 1208 (1979).
[12] G. Zerah and J. P. Hansen, J. Chem. Phys. **84**, 2336 (1985).
[13] E. Lomba, J. A. Anta, C. Martín, and M. Lombardero, Mol. Phys. **85**, 1239 (1995).
[14] P. Frodl and S. Dietrich, Phys. Rev. A **45**, 7330 (1992).

[15] C. S. Murthy, K. Singer, and I. R. McDonald, Mol. Phys. **44** (1981).

[16] F. Lado, Mol. Phys. **47**, 283–311 (1982).

[17] K. Ng, J. Chem. Phys. **61**, 2680 (1974).

[18] T. Boublik, C. Vega, and M. Díaz Peña, J. Chem. Phys. **93**, 730 (1990).

[19] M. D. Amos and G. Jackson, J. Chem. Phys. **96**, 4604 (1992).

[20] J. A. Barker and D. Henderson, J. Chem. Phys. **47**, 2856 (1967).

[21] A. Z. Panagiotopoulos, Mol. Phys. **61**, 813 (1987).

[22] P. S. Y. Cheung and J. G. Powles, Mol. Phys. **30**, 921 (1975).

[23] E. Lomba, in *Supercritical Fluids. Fundamentals for Applications*, edited by E. Kiran and J. Levelt-Sengers (Kluwer, New York, 1994).

[24] *International Critical Tables*, National Research Council (McGraw-Hill, New York, 1929).